Title

Application of Good's buffers to pH imaging using hyperpolarized 13 C MRI

Journal

Chemical Communications, 51(74)

ISSN

1359-7345

Authors

Flavell, Robert R

von Morze, Cornelius

Blecha, Joseph E

et al.

Publication Date

2015-09-25

DOI

10.1039/c5cc05348j

Peer reviewed

HHS Public Access

Author manuscript

Chem Commun (Camb). Author manuscript; available in PMC 2016 September 25.

Published in final edited form as:

Chem Commun (Camb). 2015 September 25; 51(74): 14119–14122. doi:10.1039/c5cc05348j.

Application of Good's buffers to pH imaging using hyperpolarized ^{13}C MRI

Robert R Flavell[a], **Cornelius von Morze**[a], **Joseph E. Blecha**[a], **David Korenchan**[a], **Mark Van Criekinge**[a], **Renuka Sriram**[a], **Jeremy Gordon**[a], **Hsin-Yu Chen**[a], **Sukumar Subramaniam**[a], **Robert Bok**[a], **Zhen J. Wang**[a], **Daniel Vigneron**[a], **Peder Larson**[a], **John Kurhanewicz**[a], and **David M Wilson**[a,*]

[a]Department of Radiology and Biomedical Imaging, University of California, San Francisco, California 94158, United States

Abstract

N-(2-Acetamido)-2-aminoethanesulfonic acid (ACES), one of Good's buffers, was applied to pH imaging using hyperpolarized ^{13}C magnetic resonance spectroscopy. Rapid NMR- and MRI-based pH measurements were obtained by exploiting the sensitive pH-dependence of its ^{13}C chemical shift within the physiologic range.

Metabolic reprogramming in cancer results in increased secretion of acid into the extracellular space. This results in an interstitial microenvironment that is slightly acidic, ranging from pH 6.5 – 7.0 for many cancer subtypes, in contrast with normal healthy tissue which characteristically has pH 7.2 -7.4. This property has been characterized by techniques including microelectrode measurements, magnetic resonance, and fluorescence.[1-3] Moreover, acidification of the extracellular microenvironment accompanies local invasion and metastasis in a variety of tumors.[4-6] Treatment of solid tumors with sodium bicarbonate increases tumor pH and reduces metastasis.[7] Interstitial acidity is thought to induce resistance to chemotherapeutic agents, and many small molecule agents targeting acid transporters are currently under development.[8, 9] Thus, acidic extracellular pH represents both a therapeutic target as well as a potential biomarker for the presence of aggressive cancer with higher risk of metastases.

Several magnetic resonance techniques, have been developed for the purpose of imaging acidic interstitial pH, including methods based on magnetic resonance spectroscopy (MRS) and chemical exchange saturation transfer (CEST).[6, 10-14] A central requirement for these techniques is accuracy, since the pH change between healthy and diseased tissues is small. In the MRS strategy, a probe that has a known chemical shift response to pH changes is administered systemically. The chemical shift is then measured using MRS, and by comparison to a standard curve, the pH can be determined. This approach has been studied using several different nuclei, including ^{31}P,[15-17] ^{1}H,[18-20] and ^{19}F.[21, 22] While these

*To whom correspondence should be addressed: David.m.wilson@ucsf.edu.

Electronic Supplementary Information (ESI) available: Materials and methods, supplementary figures, and characterization data for all new compounds.

techniques have provided important insights in animal model systems, they have various potential limitations, including long scan time, requirement for high dose of probe administration, and in some cases, poor spatial resolution.

Hyperpolarized ^{13}C MRS is an emerging technology which relies upon dramatic NMR signal enhancement provided *via* dynamic nuclear polarization (DNP).[23] This method has been applied to numerous chemical substrates,[24] and successfully translated to the clinic for use in men with prostate cancer.[25] An elegant pH imaging strategy using hyperpolarized ^{13}C MRS to study the equilibrium between bicarbonate and CO_2 has been reported.[26, 27] However, this technique has practical limitations, including 1) low signal to noise ratio of the CO_2 resonance under typical physiologic conditions (since $pK_{a,bicarbonate} = 6.17$), potentially propagating significant errors to pH estimates derived from this ratiometric approach, 2) the short effective T_1 relaxation time of bicarbonate *in vivo*,[26] 3) the relatively low solubility of bicarbonate in glassing agents resulting in difficulty producing sufficient polarized material, and 4) the possibility for inhibition of carbonic anhydrase,[28] which is required for rapid equilibration between bicarbonate and CO_2.

Since relative chemical shifts can in general be measured very accurately using MRS, spectroscopic, or frequency specific imaging techniques, we reasoned that a hyperpolarized ^{13}C approach employing a pair of probes with and without pH-dependent chemical shift could address some of the limitations of this prior approach. Specifically, this approach combines the robustness and high accuracy of chemical shift based MRS methods with the high signal to noise ratio inherent to hyperpolarized ^{13}C imaging.

Initially, a small library of compounds was tested with thermal equilibrium NMR, comparing ^{13}C chemical shifts of long-T_1 nuclei at pH 6.5 and 7.4 (Supplemental fig. 1). These compounds were selected based on the following key criteria: 1) pK_a near the physiologic range (between 6.0 and 8.0), 2) presence of a long T_1 nucleus, and 3) feasibility of isotopic synthesis. Agents likely to be toxic were excluded. The classes of compounds examined included biological buffers, dicarboxylic acids, and imidazole/histidine derivatives.

In his landmark 1966 paper, Dr. N. Good described criteria for an optimal biological pH buffer, and synthesized a small series of compounds which have since become the standard buffers used in biochemistry.[29] The criteria included pK_a between 6 and 8, water solubility, impermeability to biological membranes, minimum influence of temperature, concentration, or ionic strength on dissociation of the buffer, lack of binding to other biological cations, resistance to degradation, and easy synthetic preparation. We rationalized that these properties would also yield optimal pH imaging probes. Moreover, these compounds have been used widely in the 50 years since their initial description, reducing the likelihood of novel interactions which could block pH dependent chemical shift change.

Four of Good's buffers with long T_1 nuclei, and Tris, another commonly used biological buffer, are depicted in Figure 1. Of these, the compounds with the largest chemical shifts were ADA and ACES (Figure 1, Supplemental figures 2-6). In initial studies, we found that

the pH dependent chemical shift change of ADA was blocked by the presence of calcium, consistent with its known chelation properties (Supplemental table 1).[29]

Thus, we selected ACES as the most promising overall compound for imaging, due to the large pH dependant chemical shift, synthetic accessibility, predicted lack of toxicity, and known lack of chelation of abundant biological cations. ^{13}C, ^{15}N ACES was synthesized in 4 steps starting from 1-^{13}C glycine in 54% overall yield, based on the previous synthesis of the natural abundance material combined with a previously described technique for the preparation of isotopically enriched amino acids (Figure 2).[29, 30] Secondary labelling with ^{15}N was incorporated in order to eliminate low field quadrupolar T_1 relaxation effects associated with ^{14}N as well as to increase the T_2 relaxation time for imaging purposes.[31] This came at the expense of splitting of the ^{13}C peak by the spin-1/2 ^{15}N nucleus, which could potentially limit the accuracy of chemical shift measurement and signal to noise.

Since endogenous ^{13}C nuclei are not abundant enough to allow for *in vivo* imaging, we added a second compound, ^{13}C urea, as a chemical shift standard. Urea was selected since its ^{13}C chemical shift is close to that of the ACES carbonyl, and hyperpolarized ^{13}C, ^{15}N urea is a well characterized imaging agent.[32] A titration curve was developed comparing the chemical shifts of ACES and urea (Figure 3). Values for δ_{min}, δ_{max}, and pK_a were obtained by iteratively fitting the data, yielding the following equation linking chemical shift difference to pH, in a manner similar to previously described:[15]

$$pH = 6.58 - \log_{10}\frac{(\delta + 13.92)}{(-5.51 - \delta)}$$

The pK_a obtained using this technique, 6.58 (at 37 degrees), is in agreement with the previously published value of 6.56.[29]

A method for hyperpolarization of ^{13}C,^{15}N ACES was developed and optimized with respect to microwave frequency and concentration of Gd-DOTA (Supplemental table 2). The optimized prep was obtained by dissolution of ^{13}C,^{15}N ACES in 0.95 equivalents NaOH (using a 10M solution), and addition of Gd-DOTA to 0.5 mM, with 20 mM OX63 trityl radical.[33] Using this method, 12.5 ± 2.7% (n = 3) average liquid state polarization, back calculated to the time of dissolution was obtained. The T_1 was 18 s at 11.7T and 25 s at 3T. The polarization time constant was 2490 ± 396 (s.d., n= 10). A copolarization method[34] was developed to simultaneously polarize ^{13}C,^{15}N ACES and ^{13}C,^{15}N urea. By copolarizing ^{13}C,^{15}N ACES and ^{13}C,^{15}N urea, we were able to accurately determine the pH of solutions in a 500 MHz NMR (Figure 4). There was a slight but significant change in the measured pH by variation of temperature (Supplemental figure 8) and by variation of concentration of the probe (Supplemental figure 9). Furthermore, there was a slight change in the pH measured at the earliest time points in comparison to those measured at the latest time points (Supplemental figure 10). This change may be related to initial variation in temperature, and limitations of the kinetics of the acid base equilibria (although these are known to be very rapid reactions in most cases[35]). Overall, these data suggest that

the ^{13}C,^{15}N ACES and ^{13}C,^{15}N urea copolarization method could be used to determine the pH in an imaging experiment.

In order to assess the properties of this system under imaging conditions, a five compartment phantom was imaged on a clinical 3T scanner (Figure 5). Again, the dramatic chemical shift change of ACES in response to pH allowed for rapid determination of pH. There was a slight difference in pH calculated from the chemical shift and that measured on a pH meter following the experiment. These differences, averaging 0.18 pH units, may be due to a combination of factors, including temperature (supplemental figure 8), concentration (3 mM in the phantom, supplemental figure 9), the presence of phosphate buffer in the solution (supplemental table 3), or the early time point used for imaging (supplemental table 10), and are similar to previously described phantom experiments for imaging pH using hyperpolarized ^{13}C bicarbonate.[36, 37] At present, we propose that the accuracy of measured vs. calculated pH is within 0.1 – 0.2 pH units, although a much larger series of experiments would be necessary to truly estimate the accuracy (Supplemental figure 11). *In vivo* pH imaging is a key future goal for this probe. Based on the phantom experiments, we predict that injection of 0.5 mg ACES should be sufficient to generate appropriate signal to noise in a mouse, for a total dose of 25 mg/kg. Since the administered probe could potentially buffer pH, one important goal is the optimization of signal to noise ratio, as well as accuracy of the method. In order to achieve this goal, synthesis of other isotopically labelled variants is currently underway in our laboratory, including ^{14}N (to minimize signal loss due to the splitting by ^{15}N), and ^{2}H labelled probes (to improve the T_1 of the molecule).

Overall, these data demonstrate that hyperpolarized ^{13}C,^{15}N ACES can be used to determine pH using ^{13}C magnetic resonance spectroscopy. Initially, a series of compounds was screened for a large chemical shift change over the physiologically relevant pH range. Of these compounds, Good's buffers were the most promising, owing to properties considered in their initial design, coupled with the vast experience of their use. We selected ^{13}C,^{15}N ACES owing to the large chemical shift change over the physiologic range and lack of chelation properties. This compound was applied to pH measurement in an NMR spectrometer and in a chemical shift imaging experiment on a clinical 3T MRI scanner. ^{13}C,^{15}N ACES is a promising tool for imaging pH using hyperpolarized ^{13}C MRS, and we anticipate application of this probe to imaging in animal models of malignancy.

Supplementary Material

Refer to Web version on PubMed Central for supplementary material.

Acknowledgments

R.R.F. acknowledges support from NIH 5T32EB0011631-10, a University of California, San Francisco Department of Radiology Seed Grant, a Radiology Society of North America research fellow grant, and an SNMMI-ERF William and Mitzi Blahd, MD Pilot Grant. D.M.W. acknowledges support from NIH R01CA166766. C.V.M. acknowledges support from NIH K01DK099451. This project was also supported by NIH center grant P41EB013598.

Notes and references

1. Volk T, Jahde E, Fortmeyer HP, Glusenkamp KH, Rajewsky MF. Br J Cancer. 1993; 68:492–500. [PubMed: 8353039]
2. Helmlinger G, Yuan F, Dellian M, Jain RK. Nature medicine. 1997; 3:177–182.
3. Gatenby RA, Gillies RJ. Nat Rev Cancer. 2004; 4:891–899. [PubMed: 15516961]
4. Keshari KR, Sriram R, Koelsch BL, Van Criekinge M, Wilson DM, Kurhanewicz J, Wang ZJ. Cancer Res. 2013; 73:529–538. [PubMed: 23204238]
5. Estrella V, Chen T, Lloyd M, Wojtkowiak J, Cornnell HH, Ibrahim-Hashim A, Bailey K, Balagurunathan Y, Rothberg JM, Sloane BF, Johnson J, Gatenby RA, Gillies RJ. Cancer research. 2013; 73:1524–1535. [PubMed: 23288510]
6. Hashim AI, Zhang X, Wojtkowiak JW, Martinez GV, Gillies RJ. NMR Biomed. 2011; 24:582–591. [PubMed: 21387439]
7. Robey IF, Baggett BK, Kirkpatrick ND, Roe DJ, Dosescu J, Sloane BF, Hashim AI, Morse DL, Raghunand N, Gatenby RA, Gillies RJ. Cancer Res. 2009; 69:2260–2268. [PubMed: 19276390]
8. Parks SK, Chiche J, Pouyssegur J. Nat Rev Cancer. 2013; 13:611–623. [PubMed: 23969692]
9. Neri D, Supuran CT. Nature reviews Drug discovery. 2011; 10:767–777. [PubMed: 21921921]
10. Zhang X, Lin Y, Gillies RJ. Journal of nuclear medicine : official publication, Society of Nuclear Medicine. 2010; 51:1167–1170.
11. Gillies RJ, Raghunand N, Garcia-Martin ML, Gatenby RA. IEEE engineering in medicine and biology magazine : the quarterly magazine of the Engineering in Medicine & Biology Society. 2004; 23:57–64.
12. Sherry AD, Woods M. Annual review of biomedical engineering. 2008; 10:391–411.
13. Aime S, Barge A, Delli Castelli D, Fedeli F, Mortillaro A, Nielsen FU, Terreno E. Magn Reson Med. 2002; 47:639–648. [PubMed: 11948724]
14. Zhang S, Merritt M, Woessner DE, Lenkinski RE, Sherry AD. Acc Chem Res. 2003; 36:783–790. [PubMed: 14567712]
15. Gillies RJ, Liu Z, Bhujwalla Z. Am J Physiol. 1994; 267:C195–203. [PubMed: 8048479]
16. Bhujwalla ZM, McCoy CL, Glickson JD, Gillies RJ, Stubbs M. Br J Cancer. 1998; 78:606–611. [PubMed: 9744499]
17. Raghunand N, Altbach MI, van Sluis R, Baggett B, Taylor CW, Bhujwalla ZM, Gillies RJ. Biochemical pharmacology. 1999; 57:309–312. [PubMed: 9890558]
18. van Sluis R, Bhujwalla ZM, Raghunand N, Ballesteros P, Alvarez J, Cerdan S, Galons JP, Gillies RJ. Magn Reson Med. 1999; 41:743–750. [PubMed: 10332850]
19. Garcia-Martin ML, Herigault G, Remy C, Farion R, Ballesteros P, Coles JA, Cerdan S, Ziegler A. Cancer Res. 2001; 61:6524–6531. [PubMed: 11522650]
20. Provent P, Benito M, Hiba B, Farion R, Lopez-Larrubia P, Ballesteros P, Remy C, Segebarth C, Cerdan S, Coles JA, Garcia-Martin ML. Cancer Res. 2007; 67:7638–7645. [PubMed: 17699768]
21. Hunjan S, Mason RP, Mehta VD, Kulkarni PV, Aravind S, Arora V, Antich PP. Magnet Reson Med. 1998; 39:551–556.
22. Ojugo ASE, McSheehy PMJ, McIntyre DJO, McCoy C, Stubbs M, Leach MO, Judson IR, Griffiths JR. NMR Biomed. 1999; 12:495–504. [PubMed: 10668042]
23. Ardenkjaer-Larsen JH, Fridlund B, Gram A, Hansson G, Hansson L, Lerche MH, Servin R, Thaning M, Golman K. Proc Natl Acad Sci U S A. 2003; 100:10158–10163. [PubMed: 12930897]
24. Keshari KR, Wilson DM. Chem Soc Rev. 2014; 43:1627–1659. [PubMed: 24363044]
25. Nelson SJ, Kurhanewicz J, Vigneron DB, Larson PE, Harzstark AL, Ferrone M, van Criekinge M, Chang JW, Bok R, Park I, Reed G, Carvajal L, Small EJ, Munster P, Weinberg VK, Ardenkjaer-Larsen JH, Chen AP, Hurd RE, Odegardstuen LI, Robb FJ, Tropp J, Murray JA. Sci Transl Med. 2013; 5:198ra108.
26. Gallagher FA, Kettunen MI, Day SE, Hu DE, Ardenkjaer-Larsen JH, Zandt R, Jensen PR, Karlsson M, Golman K, Lerche MH, Brindle KM. Nature. 2008; 453:940–943. [PubMed: 18509335]

27. Lau AZ, Chen AP, Ghugre NR, Ramanan V, Lam WW, Connelly KA, Wright GA, Cunningham CH. Magn Reson Med. 2010; 64:1323–1331. [PubMed: 20574989]
28. Schroeder MA, Swietach P, Atherton HJ, Gallagher FA, Lee P, Radda GK, Clarke K, Tyler DJ. Cardiovasc Res. 2010; 86:82–91. [PubMed: 20008827]
29. Good NE, Winget GD, Winter W, Connolly TN, Izawa S, Singh RM. Biochemistry. 1966; 5:467–477. [PubMed: 5942950]
30. Grehn L, Bondesson U, Pehk T, Ragnarsson U. J Chem Soc Chem Comm. 1992:1332–1333.10.1039/C39920001332
31. Reed GD, von Morze C, Bok R, Koelsch BL, Van Criekinge M, Smith KJ, Hong S, Larson PE, Kurhanewicz J, Vigneron DB. IEEE transactions on medical imaging. 2014; 33:362–371. [PubMed: 24235273]
32. von Morze C, Larson PEZ, Hu S, Keshari K, Wilson DM, Ardenkjaer-Larsen JH, Goga A, Bok R, Kurhanewicz J, Vigneron DB. Journal of Magnetic Resonance Imaging. 2011; 33:692–697. [PubMed: 21563254]
33. Ardenkjaer-Larsen JH, Macholl S, Johannesson H. Appl Magn Reson. 2008; 34:509–522.
34. Wilson DM, Keshari KR, Larson PE, Chen AP, Hu S, Van Criekinge M, Bok R, Nelson SJ, Macdonald JM, Vigneron DB, Kurhanewicz J. J Magn Reson. 2010; 205:141–147. [PubMed: 20478721]
35. Eigen M. Angewandte Chemie International Edition in English. 1964; 3:1–19.
36. Ghosh RK, Kadlecek SJ, Pourfathi M, Rizi RR. Magn Reson Med. 201410.1002/mrm.25530
37. Lee Y, Zacharias NM, Piwnica-Worms D, Bhattacharya PK. Chem Commun (Camb). 2014; 50:13030–13033. [PubMed: 25224323]

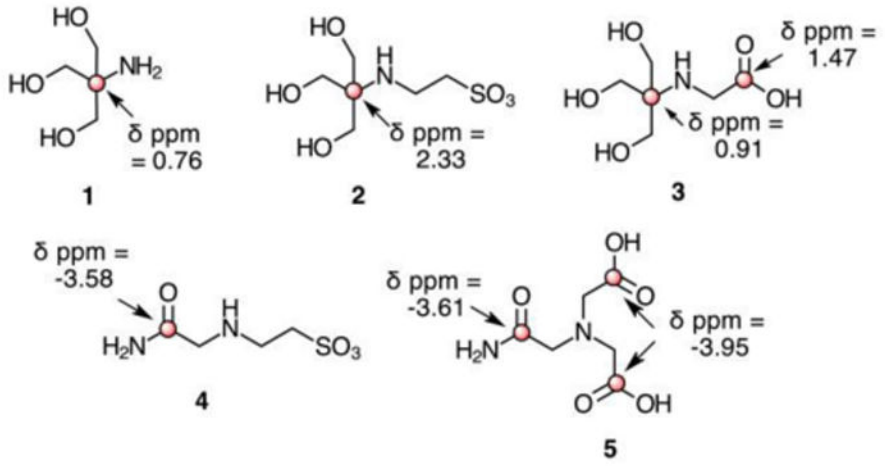

Compound	Trivial name	pKa (37°)	δ, pH 6.5	δ, pH 7.4
1	Tris	7.72	65.1	64.37
2	TES	7.16	65.57	63.24
3	Tricine	7.8	171.76, 65.53	173.22, 64.61
4	ACES	6.56	174.02	177.6
5	ADA	6.46	174.95, 173.34	178.56, 177.29

Fig. 1.

Structures of Good's buffers. Long T_1 nuclei are indicated in red. The difference in chemical shift between pH 6.5 and 7.4 is shown for long T_1 nuclei. A positive δ ppm indicates a downfield ^{13}C chemical shift. pKa are based on prior literature values.

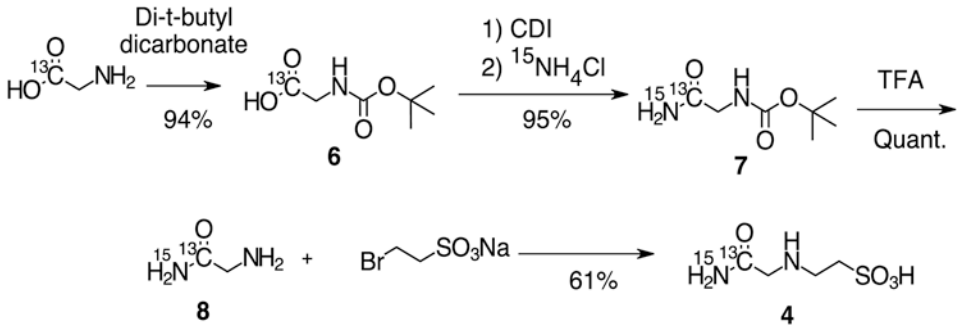

Fig 2.
Synthesis of ^{13}C, ^{15}N, ^{13}C ACES.

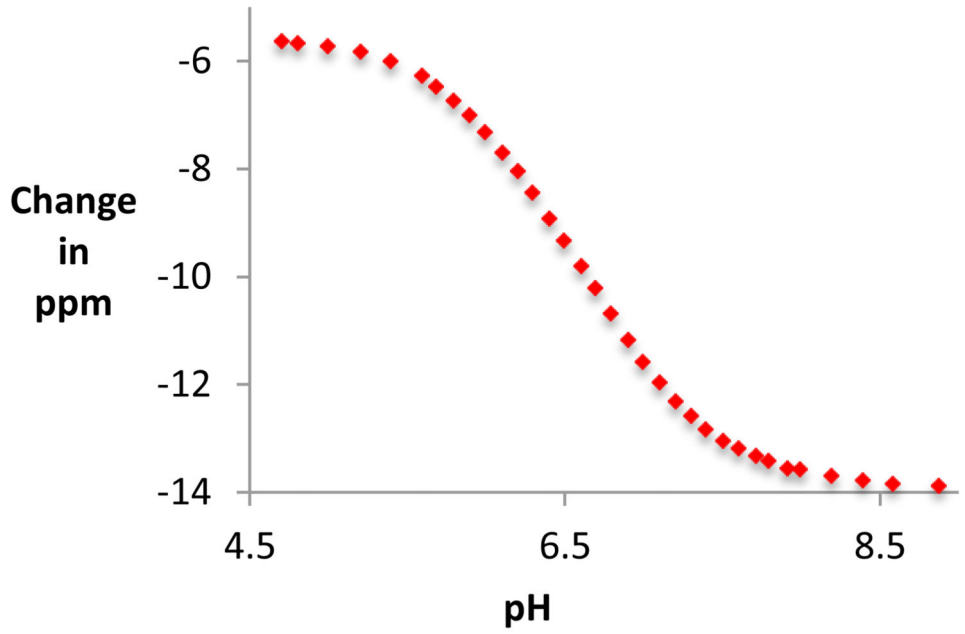

Figure 3.
Titration curve depicting the difference in chemical shift between urea and ACES as a function of pH.

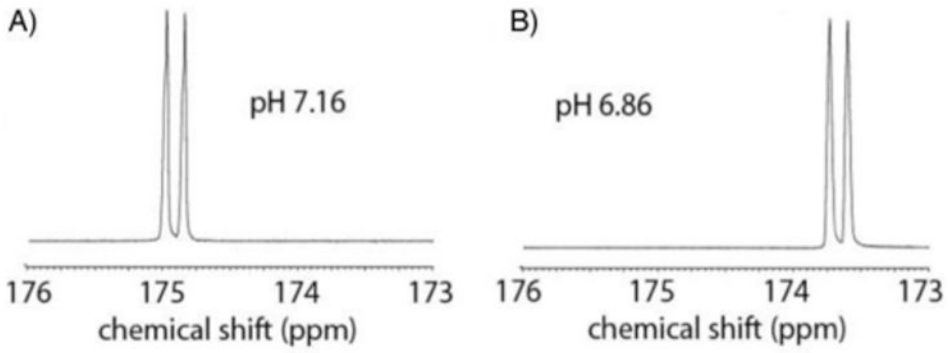

Figure 4.

Measurement of pH with $^{13}C,^{15}N$ ACES. The calculated pH values of 7.16 and 6.86 correlated with the values of 7.22 and 6.91 measured on a pH meter following the experiment. The carboxylate of $^{13}C,^{15}N$ ACES is a doublet owing to coupling with the adjacent ^{15}N.

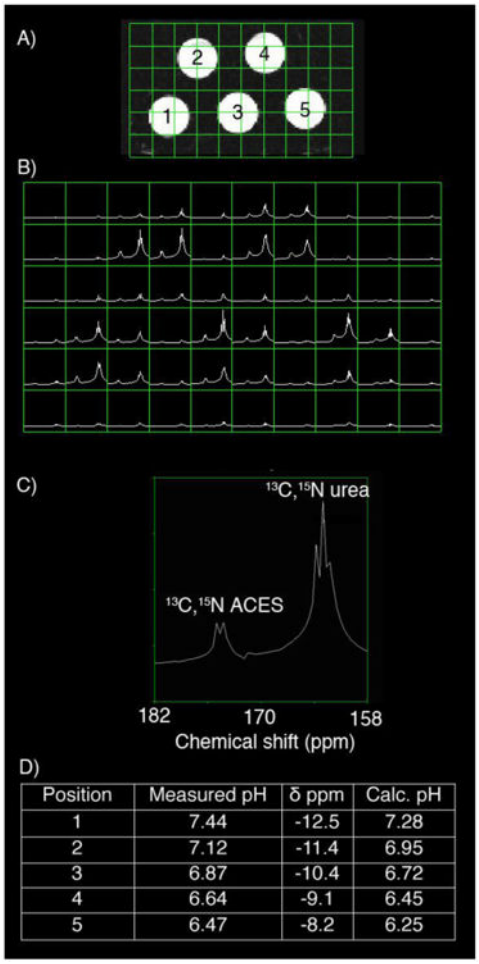

Position	Measured pH	δ ppm	Calc. pH
1	7.44	-12.5	7.28
2	7.12	-11.4	6.95
3	6.87	-10.4	6.72
4	6.64	-9.1	6.45
5	6.47	-8.2	6.25

Figure 5.

Five compartment phantom for imaging pH using ^{13}C, ^{15}N ACES and ^{13}C,^{15}N urea A) Phantom design incorporated 5 compartments with varying pH. B) 2D chemical shift imaging through the phantom. C) Representative voxel from position 2. D) Summary of calculated and measured pH values.